JOURNAL OF MAGNETIC RESONANCE **130,** 253–261 (1998)
ARTICLE NO. MN971307

Influence of High Orientational Order on the Shape of the Echo Response from a Hahn Pulse Sequence

C. van der Struijf,* H. K. Nienhuys,* D. Harryvan,*,† G. Kothe,† and Y. K. Levine*,[1]

*Debye Institute, Buys Ballot Laboratory, P.O. Box 80.000, 3508 TA Utrecht, The Netherlands; and †Department of Physical Chemistry, University of Freiburg, Albertstrasse 21, D-79104 Freiburg, Germany

Received May 2, 1997

The amplitude modulations in the simulations of the Hahn echo responses from cholestane spin labels in samples characterized by a high degree of orientational order are shown to arise from the use of ''soft'' pulses. Soft pulses have a limited spectral range and cover only a small portion of the CW-ESR spectra, so that not all the spins are on-resonance. The magnetization vectors of the off-resonance spins only partially tilted away from the laboratory *z* axis, the direction of the applied static magnetic field. They thus contribute oscillating components to the magnetization in the *xy* plane. The contribution from the off-resonance spins to the Hahn echo formation is significant in highly oriented samples, but cancels out in samples exhibiting a small degree of order. Experimental echo responses obtained from CSL molecules embedded in rigid matrices of eggPC bilayers and the liquid crystalline materials ZLI and MBBA confirm the theoretical predictions.

INTRODUCTION

Two-dimensional electron-spin-echo (2D-ESE) techniques are known to be suitable for the study of rotational motions on the microsecond time scale (*1*). In this way it is possible to characterize the motional behavior of nitroxide spin labels attached to the large membrane protein Ca-ATPase incorporated in lipid bilayers. The Ca-ATPase molecules are generally believed to be embedded in lipid bilayers with their long axes perpendicular to the bilayer plane (*2*). The planes of the bilayers are, however, isotropically distributed in space. In these 2D-ESE experiments, the Hahn pulse sequence ($\pi/2-\tau-\pi$) is used to produce an echo of amplitude $E(\boldsymbol{B}_0, \tau)$ at time τ following the second pulse as a function of the interpulse time. The ''soft'' microwave pulses are applied at a magnetic field position $\boldsymbol{B}_0$ within the CW-ESR absorption spectrum. The slow motions of the nitroxide-labeled protein cause an irreversible loss of coherence during the interpulse time, resulting in a decay of the echo amplitude. The information about the motion is contained in the decay rate and its variation across the CW-ESR absorption spectrum.However, this information can only be extracted quantitatively through numerical simulation techniques.

We have recently shown that the echo responses elicited by the Hahn sequence utilizing soft microwave pulses can be evaluated in the time domain by solving the Bloch equations for the stochastic spin Hamiltonian on making use of stochastic trajectories for the orientational behavior of the spin-labeled protein (*1*). This approach rests on the observation that in the ultraslow motion regime, the resonance frequencies in the pseudo-secular approximation are fully determined by the orientation of the nitroxides relative to $\boldsymbol{B}_0$. The central step in the simulations involves the computation of the echo response from spin-labeled proteins with a given orientation relative to the applied static magnetic field $\boldsymbol{B}_0$. The echo responses computed for a large ensemble of molecules with different spatial orientations are then summed in order to mimic the experimental signal.

Interestingly, the echo responses simulated for a given orientation of the Ca-ATPase were often characterized by amplitude modulations (*1*). These modulations, however, were averaged out in the simulated response from the random assembly of spin-labeled proteins. Interestingly, the modulations could also be removed by the application of a phase cycling procedure, which resulted in normal echo responses similar to those calculated for a randomly oriented sample.

In this paper we shall address the origin of the amplitude modulations in the simulations of the Hahn echo responses from samples characterized by a high degree of orientational order. Furthermore, we shall present experimental evidence to support the predictions from the simulations. To this end CSL molecules were embedded in rigid matrices of eggPC bilayers and the liquid crystalline materials ZLI and MBBA (*3*).

It will be shown below that the modulations arise from the use of soft pulses in the Hahn sequence. Soft pulses have a limited spectral range and cover only a small portion of the CW-ESR spectra, so that not all the spins are on-resonance. The magnetization vectors of the off-resonance spins only partially tilted away from the laboratory *z* axis, the

[1] To whom correspondence should be addressed.

1090-7807/98 $25.00

direction of the applied static magnetic field. They thus contribute oscillating components to the magnetization in the *xy* plane. The contribution from the off-resonance spins to the Hahn echo formation is significant in highly oriented samples, but cancels out in samples exhibiting a small degree of order. The experimental echo responses obtained from CSL molecules embedded in rigid matrices of eggPC bilayers and the liquid crystalline materials ZLI and MBBA confirm the theoretical predictions.

MATERIALS AND METHODS

EggPC was obtained from Sigma and used without further purification. EggPC is a mixture of fatty acids, containing mostly stearic and oleic fatty acids (*4*). The spin label 4′,4′-dimethylspiro[5α-cholestane-3,2′-oxyzolidin]-3′-yloxy (CSL) was obtained from Aldrich and used without further purification.

In all the samples a CSL concentration of 1 mol% was used. At this concentration, the spin–spin interactions between individual CSL molecules are expected to produce homogeneous line broadening of approximately 0.5 G. This value is smaller than the combined effects of Lorentzian and Gaussian broadening, about 2.5 G.

EggPC/CSL mixtures were prepared by dissolving the components in chloroform. After mixing, the chloroform was removed by a flow of nitrogen gas and the mixtures were equilibrated over a saturated K_2SO_4 solution for more than 16 h. The eggPC/CSL mixtures prepared in this way contained about 24 wt% water (*5*). The oriented samples were obtained in the following way. The egg/CSL mixture was oriented between glass plates (3×5 mm) by the application of shear pressure. The macroscopic alignment of the bilayers was checked optically with a polarizing microscope equipped with a first-order red plate. Ten to fourteen individual samples were stacked in order to improve the signal-to-noise ratio.

The aligned samples of CSL in a liquid crystalline matrix were prepared in the following way. ZLI 85-1084 was obtained from Merck and used without further purification. This material exhibits a smectic–nematic transition at 233 K and a clearing temperature at 334 K (*6*). One millimolar CSL was added to ZLI 85-1084 in a quartz tube with an inner diameter of 2 mm. The sample was heated above the clearing point temperature and placed in a magnetic field of 1.4 T in order to align the liquid crystalline phases of ZLI. The ZLI matrix imposes an orientation on the CSL molecules in the direction of the magnetic field. The sample was then cooled down at a rate of 2 K/min to the crystalline phase. After reaching the crystalline phase the magnetic field was switched off. In this way, the CSL probes are frozen into the aligned crystalline matrix and the oriented sample can be rotated in the resonator without disturbing the orientational distribution of CSL.

Unoriented samples were prepared by dissolving CSL in *p*-methoxy-benzylidine-*p*-*n*-butylaniline (MBBA). This liquid crystalline material was obtained from Merck and used without further purification. MBBA has a clearing temperature of 317 K and a crystalline phase below 202 K (*7*).

The CW-ESR measurements were carried out on a Bruker ESP-300 operating at X-band frequency, employing 100 kHz field modulation. The modulation amplitude was about 1 G and power levels of the microwave frequency were well below saturation. The alignment of the sample relative to the static magnetic field was controlled with a homebuilt goniometer with an accuracy of $\pm 1°$.

The echo shape measurements on eggPC/CSL samples were carried out on an X-band Bruker ESP-300 spectrometer equipped with a homebuilt pulsed ESR bridge. The lipid bilayer sample was placed in a bridged loop 2 gap resonator (*8*), which is critical coupled to the waveguide. Such a resonator has the advantage that the sample can be rotated without affecting the resonance frequency of the resonator and the critical coupling to the waveguide.

About 3 W of pulse power was coupled into the resonator, resulting in $\pi/2$ pulse lengths of 40 ns. The resonator had a typical bandwidth of about 40 MHz and a quality factor (*9*) of about 300.

The time-dependent signals were captured with a Lecroy 9450 oscilloscope. The integrated echo intensity was accumulated for 400 pulse sequences at each field position $\boldsymbol{B}_0$ and interpulse time τ and subsequently stored for further analysis.

The lipid bilayer samples were cooled with liquid nitrogen and the temperature was controlled within 1 K with a Bruker ER-4111 VT.

The echo shape measurements on the CSL/liquid crystalline samples were carried out on an X-band Bruker ESP-380 spectrometer. The sample quartz tube was placed in a split-ring resonator (*10*) and the alignment of the sample relative to the magnetic field was determined by a homebuilt goniometer. The split-ring resonator in the overcoupled mode was used in conjunction with a 1-kW TWT amplifier of the microwave power of a klystron, resulting in a quality factor of about 300 and $\pi/2$ pulse lengths of 40 nsec.

The temperature was controlled with a helium cryostat from Oxford.

All the experiments were carried out at 160 K.

THEORETICAL ANALYSIS

Orientational Order

The first step in the description of the behavior of the CSL molecules in the lipid and liquid crystalline matrices is the generation of a trajectory of their stochastic orientation in the system as a function of time. The orientation of the CSL is fully characterized by the set of three Euler angles

$\Omega \equiv \{\alpha, \beta, \gamma\}$ (*11*). The Z axis of the frame in which Ω is defined is taken to be the director of the sample. In the eggPC samples, the director is the normal to the bilayer planes, while in the ZLI samples it is the direction of the magnetic field $\boldsymbol{B}_0$ during the thermal quench.

The orientational distribution of CSL in the samples is most conveniently described in terms of a Boltzmann orientational distribution function $f(\Omega)$ corresponding to an orienting potential $U(\Omega)$. The distribution defines the relative probability of finding a molecule at an orientation $\Omega + d\Omega$, where $d\Omega \equiv \sin\beta d\alpha d\beta d\gamma$. This distribution function is taken to be cylindrically symmetric around the director axis of the lipid bilayer or the liquid crystal matrix: The simplest distribution function $f(\Omega)$ takes the form (*5*)

$$U(\Omega) = -kT\{\lambda_2 P_2[\cos(\beta - \kappa)]\}$$
$$f(\Omega) = f(\beta) = \exp\{\lambda_2 P_2[\cos(\beta - \kappa)]\}, \qquad [1]$$

where P_2 denotes the Legendre polynomials of order 2,

$$P_2(\cos\beta') = \tfrac{1}{2}(3\cos^2\beta' - 1), \qquad [2]$$

and κ is the angle between the director and the axis of the orienting potential. The degree of alignment along the director is commonly characterized by the order parameter $\langle P_2\rangle$:

$$\langle P_2\rangle = \frac{1}{N}\int_0^\infty d\beta \sin\beta f(\beta) P_2(\cos\beta). \qquad [3]$$

Note that $\langle P_2\rangle \equiv 0$ for a randomly oriented, or unoriented, sample while $\langle P_2\rangle \equiv 1$ when the molecules are perfectly aligned along the director.

CW-ESR Spectral Simulations

We shall here be concerned only with ultraslow motions of the nitroxide labels on the microsecond time scale. In this regime the CW-ESR spectral lineshapes are not modulated by motion and are affected only by the magnetic interactions. We shall therefore omit the time dependence of the Hamiltonian H in the simulations. The effects of motion can be included in a straightforward way as described previously (*12*).

The spin Hamiltonian H is (*13*)

$$H = \boldsymbol{B}_0 \cdot \mathbf{g}(\Omega) \cdot S_z + I \cdot \mathbf{A}(\Omega) \cdot S_z, \qquad [4]$$

where $\boldsymbol{B}_0$ is the static magnetic field, S is the electron spin, I is the nuclear spin, $\mathbf{g}(\Omega)$ is the anisotropic electron g tensor, and $\mathbf{A}(\Omega)$ is the anisotropic electron-nuclear hyperfine tensor. The magnetic tensor elements in the principal frame, which coincides with the molecular frame, are (*5*)

$$\mathbf{A} = \begin{pmatrix} 5.6 & 0 & 0 \\ 0 & 34.0 & 0 \\ 0 & 0 & 5.3 \end{pmatrix} \qquad [5]$$

$$\mathbf{g} = \begin{pmatrix} 2.0081 & 0 & 0 \\ 0 & 2.0024 & 0 \\ 0 & 0 & 2.0061 \end{pmatrix}. \qquad [6]$$

The tensor components in the laboratory frame are calculated using standard rotational transformations (*11*). The resonance frequency of a nitroxide label, ω_{res}, is now fully defined in terms of its instantaneous orientation and is easily obtained in the pseudo-secular approximation on diagonalizing the spin Hamiltonian (*14, 15*).

The simulation of the CW-ESR spectral lineshape involves a simple summation of stick spectra over the ensemble of molecular orientations. Homogeneous (*16*) and inhomogeneous (*17*) line-broadening effects are superimposed on the final spectrum by a convolution procedure. Typically, the intrinsic Lorentzian linewidth was 0.5 G and the Gaussian broadening variance was 2.5 G. The first derivative of the absorption spectrum is calculated in the time domain using Fourier transformation algorithms (*18*). This procedure yields robust numerical simulations. Stable spectral lineshape simulations for unoriented samples were obtained using an ensemble of 15,000 molecules and took 2 s CPU time on a DEC3100 workstation.

Typical spectral lineshapes for an oriented sample with its director lying parallel and perpendicular to the static magnetic field $\boldsymbol{B}_0$ are shown in Fig. 1. The figure illustrates the effect of the orientational order on the spectral lineshapes for the two positions of the director relative to $\boldsymbol{B}_0$. The two spectra are identical for an orientationally unoriented sample, $\langle P_2\rangle = 0$. While the spectral features found with the director perpendicular to $\boldsymbol{B}_0$ only sharpen as $\langle P_2\rangle$ increases from 0 to 1, the spectral lineshapes obtained with the director parallel to $\boldsymbol{B}_0$ narrow and change shape.

The purpose of the simulations is to extract the order parameters of the nitroxide label in the sample by reproducing the experimental spectra. Thus in practice, a search procedure is implemented whereby the input order parameter is varied and the quality of the agreement between the experimental and simulated spectra is judged visually. It is important to note now that the direction of the orienting potential acting on the nitroxide labels need not necessarily coincide with the sample director. Indeed, we expect the direction of the orienting director to be tilted relative to the planes of the lipid bilayers. The reason for this is that the CSL molecules are intercalated between the hydrocarbon chains of the lipid, which are known to be tilted relative to the bilayer surface at low temperature (*19*). Such a tilt can be deduced simply from the variation of the lineshape with the sample orientation relative to $\boldsymbol{B}_0$ and is taken into account in the analysis of the spectra.

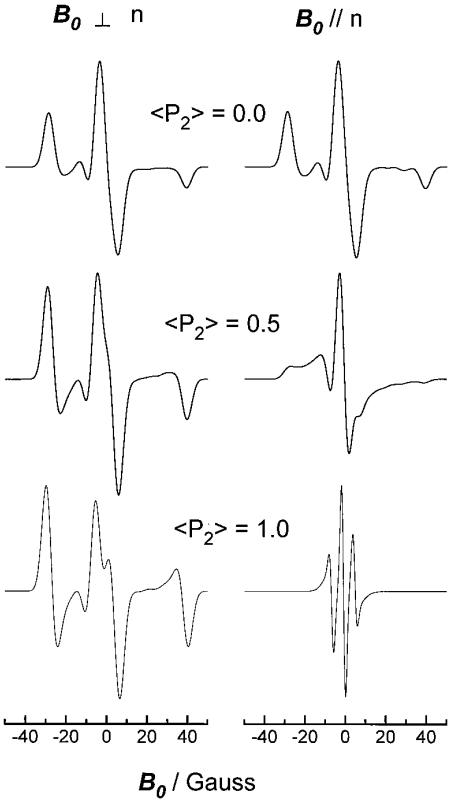

FIG. 1. The CW spectral lineshapes of nitroxide spin labels with $\boldsymbol{B}_0$ oriented perpendicular and parallel to the director n. The magnetic field position is shown relative to the central peak.

Simulation of Echo Responses to the Hahn Pulse Sequence

The time evolution of spins is subjected to the Hahn pulse sequence (*20*):

$$\left(\frac{\pi}{2}\right)_x - \tau - (\pi)_x - \text{acquire}_y. \qquad [7]$$

The numerical simulations of the echo response essentially follow the protocol described in (*1*) and only the salient points will be summarized here. The evolution of the magnetization under influence of the microwave pulses is evaluated by considering each pulse to consist of a series of elementary pulses of duration Δt. Here Δt is of the order of 1 ns, corresponding to a rotation of the magnetization about the microwave field $\boldsymbol{B}_1$ of 2°. Following each of these elementary pulses, the magnetization of the nitroxide molecule is allowed to precess about $\boldsymbol{B}_0$ with a frequency $\omega_{\text{precess}} = \omega_{\text{res}}(\Omega) - \gamma_e \boldsymbol{B}_0$. The resonance frequency is calculated using the trajectory of stochastic orientations and is updated after every elementary pulse to take account of reorientational motions. In the absence of the microwave field, the same procedure of dividing the time into time steps of duration Δt is used. Only in this case is there no rotation about the microwave field $\boldsymbol{B}_1$. The computed echo responses showed no dependence on the length of this time step in the cases considered here. Stable echo responses were computed using 15,000 molecules, and no significant improvement was achieved by increasing this number. In order to facilitate a comparison with experiments, the echo responses obtained from the simulations were corrected for the 40-MHz bandwidth of the resonator by numerical filtering in the frequency domain. Similarly as the homogeneous and inhomogeneous broadening effects smooth out the amplitude modulations, they were also only included for purposes of comparing the simulations with experimental echo responses.

In order to understand the origin of the amplitude modulations of the echo responses, we shall first consider simulations of a random distribution of nitroxide labels undergoing rotations about their long axes, $\langle P_2 \rangle = 0$. In doing this it is necessary to recognize that only spins whose precession frequencies lie within a narrow band centered around the frequency of the applied microwave field are fully rotated into the *xy* plane. Spins with precession frequencies outside this band will be only partially rotated by the microwave pulses.Their magnetization components in the *xy* plane may thus contribute to the echo form. It is usually assumed that the magnetization vectors of all the different off-resonance spins cancel out in the *xy* plane, such that they do not contribute to the echo signal from the on-resonance spins.

The contribution of the on- and off-resonance spins to the echo response of a random distribution of nitroxide labels is illustrated in Fig. 2. The pulse sequence was applied in the middle of the CW-ESR spectrum with a $\pi/2$ pulse length of 40 ns and an interpulse time τ of 300 ns. The time evolution of the magnetization vectors of spins lying in a range of 35 G around $\boldsymbol{B}_0$ was simulated. For ease of computation, the CW-ESR spectrum was divided into 71 bins each of width 0.1 G.

A stereographic view of the spatial orientation of the magnetization vectors directly after the $\pi/2$ pulse is shown Fig. 2A. Note that the magnetic field $\boldsymbol{B}_0$ defines the *z* axis. It can be seen that the greatest portion of the magnetization vectors remain parallel to the *z* axis, and only a small portion has been tilted away from $\boldsymbol{B}_0$ by the pulse. The distribution of the magnetization components in the *xy* plane is shown Fig. 2B. The corresponding distributions of magnetizations at the moment of echo formation are shown in Figs. 2C and 2D. As a guide to the eye, a dashed line has been included in the figures joining magnetization vectors whose resonance frequencies lie within a band of width $\omega_{\text{Rabi}} = \gamma_e \boldsymbol{B}_1$ around the microwave frequency. It can be seen that the distribution of magnetization vectors in the *xy* plane is highly symmetric, leading to an exact cancellation of the signals from the off-resonance spins. Thus only the magnetization vectors of the on-resonance spins add up coherently to form an echo signal.

In marked contrast to the case of a randomly oriented sam-

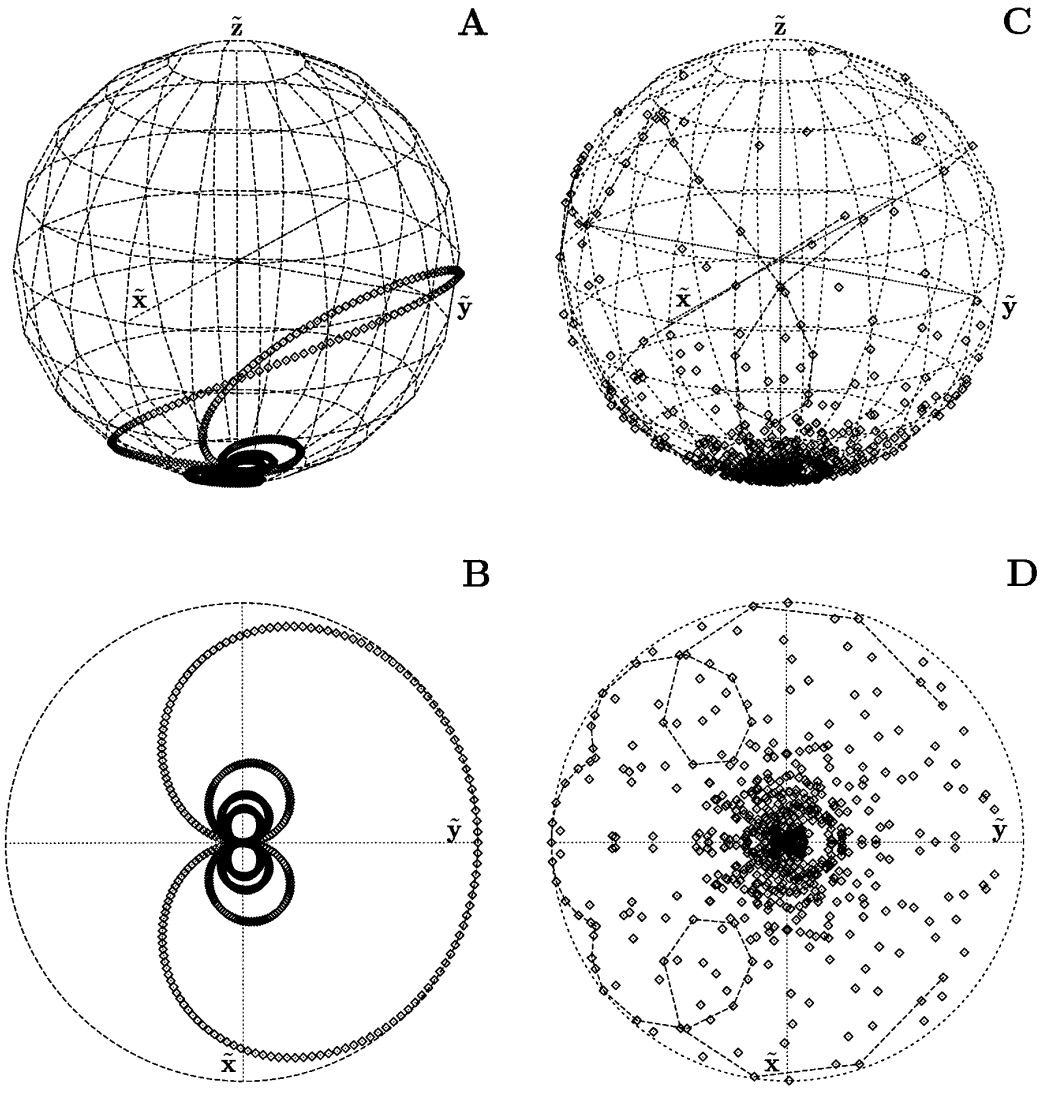

FIG. 2. A stereographic view of the directions of the magnetization vectors during a Hahn pulse experiment: ◇ represents the position of the tip of a spin vector with a specific resonance frequency. (A) The distribution of the magnetization vectors over the surface of a unit sphere whose z axis is $\boldsymbol{B}_0$ directly after a $\pi/2$ pulse; (B) projection of the magnetization vectors in **A** on the xy plane; (C) as in **A,** but at the instant of the formation of the echo maximum; (D) projection of the magnetization vectors in **C** on the xy plane.

ple, no exact cancellation of the magnetization components of the off-resonance spins is possible in a sample exhibiting a high orientational order, $\langle P_2 \rangle \approx 1$. As can be seen from the CW-ESR spectrum, Fig. 1, the spins are essentially found in three packets with well-defined precession frequencies. The magnetization components in the xy plane now consist of a superposition of three oscillating components, which are asymmetrically distributed in the plane. The contributions from the off-resonance spin packets are expected to cancel out identically only by a judicious choice of the magnetic field position at which the Hahn sequence is applied. In other words, a cancellation of the contributions of the off-resonance spins to the echo signal requires their magnetization components to be distributed symmetrically over the xy plane.

We shall now consider the echo responses elicited by the Hahn pulse sequence from samples in which the nitroxide molecules are either tilted relative to $\boldsymbol{B}_0$ or exhibit an orientational distribution. The simulations covered only the low- and center-field line of the CW-ESR spectrum as the result of an unsatisfactorily low signal intensity in the high-field line. It is important to note that a low signal-to-noise ratio in the high-field line of the spectrum is also found experimentally (*1*). The central peak was set at 3373 G, as found for the eggPC/CSL samples, and neither filtering of frequency components nor Gaussian broadening effects were included in these simulations.

The Hahn echo responses obtained from perfectly oriented nitroxide labels whose Z axes all lie at an angle β

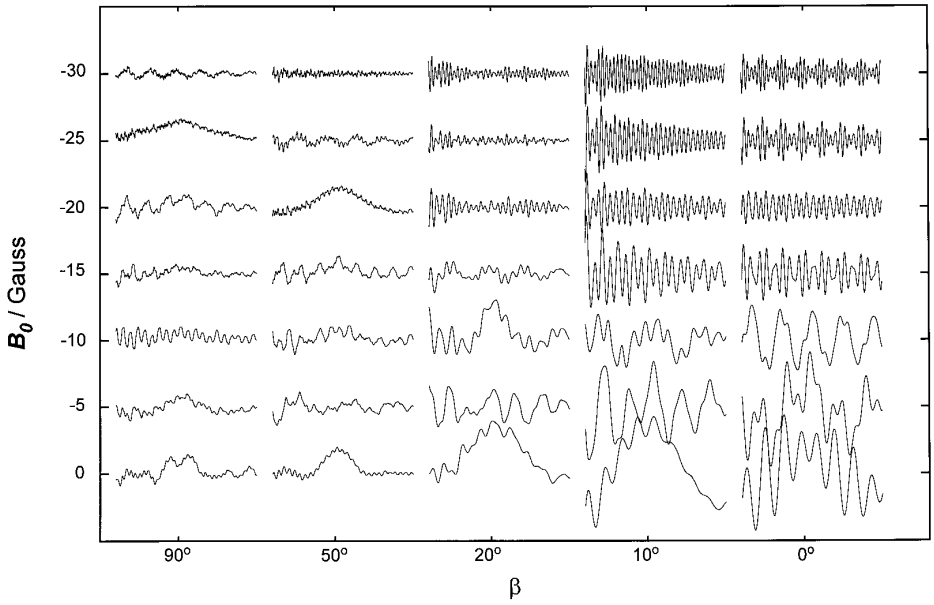

FIG. 3. Simulated echo shapes from perfectly aligned nitroxide molecules whose axes lie at an angle β relative to the director at different magnetic field positions. The field position is given relative to the central peak and only the low-field portion is shown. Every trace is an echo shape, with horizontally a time window around the echo maximum (450 ns) and vertically the magnetization along the y axis.

relative to $\boldsymbol{B}_0$ are shown in Fig. 3. Note that the X and Y axes undertake random orientations. The echo responses were computed for a period of 450 ns following the application of the second π pulse of the Hahn sequence as a function of orientation and field position. An interpulse time of 300 ns was used. It can be clearly seen from Fig. 3 that the extent of the modulation of the signals is particularly strong when the nitroxide molecules lie with their Z axes along $\boldsymbol{B}_0$. However, the depth of the modulations weaken significantly as the orientation of the nitroxide axis relative to $\boldsymbol{B}_0$ increases from $\beta = 0$ to $\beta = 90°$, when Z axes of the nitroxides lie at right angles to

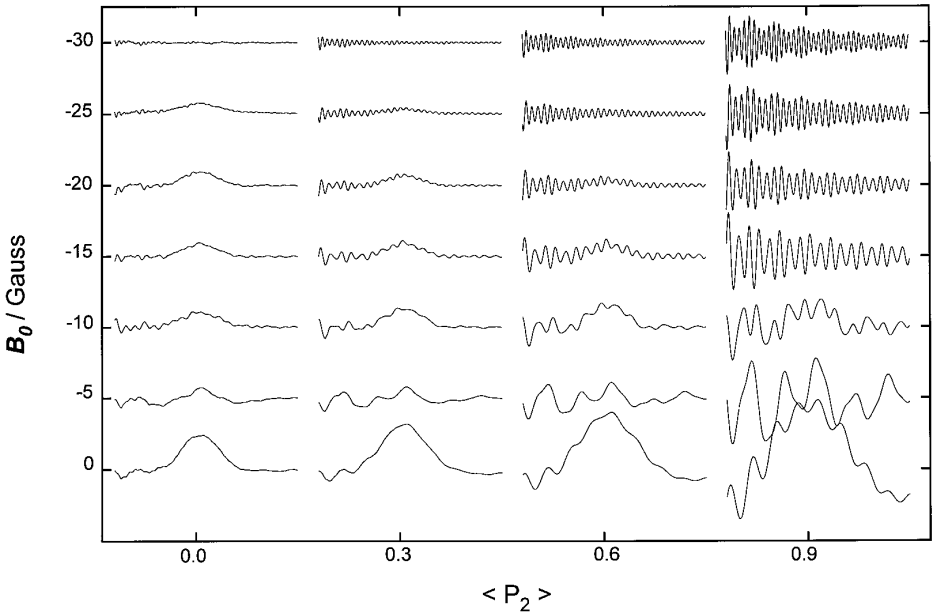

FIG. 4. Simulated echo forms as in Fig. 3, but for different values of $\langle P_2 \rangle$ and magnetic field positions.

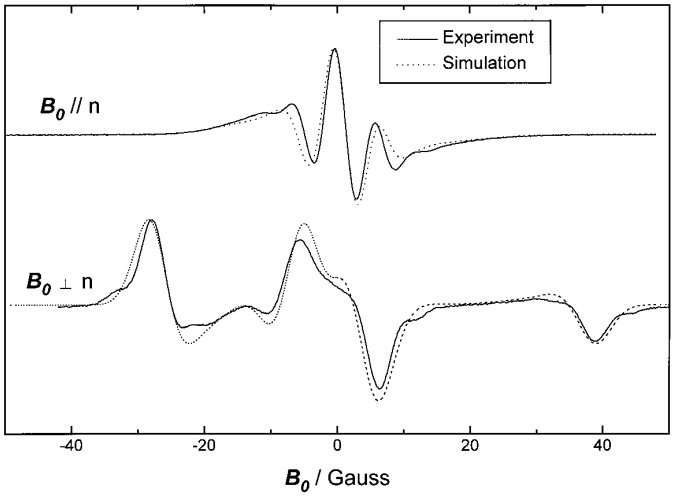

FIG. 5. CW-ESR spectra of ZLI 85-1084 at $T = 160$ K. Shown are the experimental data (solid lines) and the best fit as judged by a visual inspection (dashed line) obtained with $\boldsymbol{B}_0$ oriented parallel and perpendicular to the sample director n.

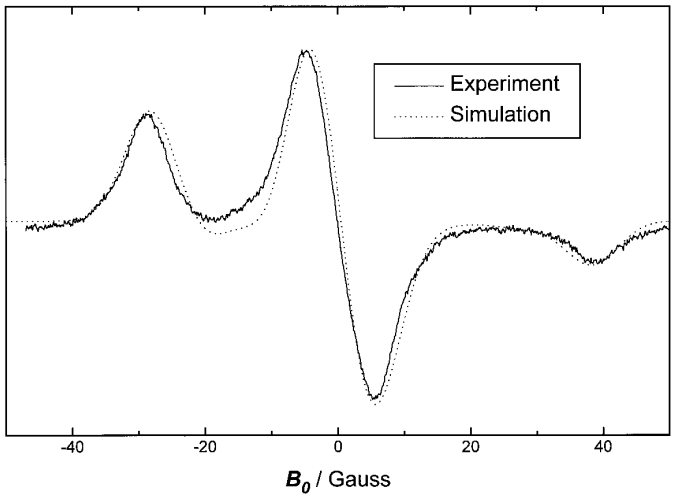

FIG. 6. CW-ESR spectra of MBBA at $T = 160$ K. Shown are the experimental data (solid line) and the best fit judged by visual inspection (dashed line) found at every orientation of the sample director n relative to $\boldsymbol{B}_0$.

the field. Interestingly, the nitroxide labels whose axes lie almost parallel to $\boldsymbol{B}_0$, $\beta \approx 0$, exhibit responses strongly resembling an echo shape at fields near the center of the spectrum, i.e., $\boldsymbol{B}_0 \approx 3373$ G.

The modulations in the responses smooth out considerably when the Z axes of the nitroxide label undertake a distribution of orientations relative to $\boldsymbol{B}_0$, Fig. 4. The orienting potential was taken to lie parallel to $\boldsymbol{B}_0$ in all the cases shown. The smoothing of the modulations depends strongly on the width of the orientational distribution as expressed in terms of the order parameter $\langle P_2 \rangle$: the lower the orientational order the smoother the response. This underpins the conclusions reached in the discussion above.

EXPERIMENTAL RESULTS AND DISCUSSION

CW-ESR Absorption Spectrum

The CW-ESR spectra obtained from oriented samples of ZLI 85-1084 at 160 K, Fig. 5, indicate a marked degree of orientational order of the CSL molecules. This is evidenced by the differences in the spectral lineshapes observed with the director oriented parallel and perpendicular to $\boldsymbol{B}_0$. Also shown in Fig. 5 are the best fits to the lineshapes judged by visual inspection. The extracted values for $\langle P_2 \rangle$ and the tilt angle κ of the orienting potential relative to the director are given in Table 1. In contrast to ZLI 85-1084, a random distribution of CSL molecules is found in the MBBA matrices, Fig. 6. However, the CSL molecules exhibit a significantly higher degree of orientational order in the eggPC matrices than in the ZLI matrices, Fig. 7 and Table 1. The tilt angle of the nitroxide labels relative to the bilayer planes corresponds well with

TABLE 1
Values of the Fit Parameters $\langle P_2 \rangle$ and Tilt Angle Extracted from the Fits of the CW-ESR Spectra

Sample	$\langle P_2 \rangle$	κ
EggPC/CSL	0.95 ± 0.04	29° ± 5°
ZLI 85-1084/CSL	0.70 ± 0.03	10° ± 5°
MBBA/CSL	0	0° ± 5°

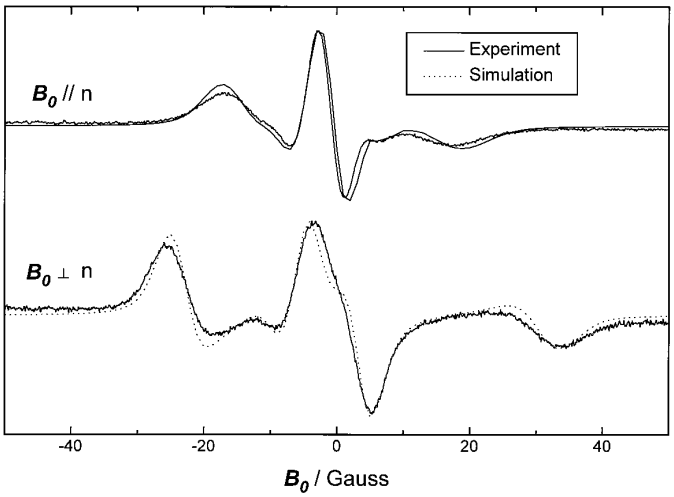

FIG. 7. CW-ESR spectra of eggPC at $T = 160$ K. Shown are the experimental data (dashed lines) and the best fit as judged by a visual inspection (solid line) obtained with $\boldsymbol{B}_0$ oriented parallel and perpendicular to the sample director n.

the tilt of the hydrocarbon chains observed in X-ray diffraction experiments on lipid bilayers in the low temperature hydrated crystalline phase (*19*).

Echo Shapes

Typical echo responses from CSL in the ZLI matrices are shown in Fig. 8 with the magnetic field $\boldsymbol{B}_0$ parallel to the sample director. The response for the parallel orientation compares favorably with the theoretical responses calculated with $\langle P_2 \rangle = 0.6$ and shown in Fig. 4. It is important to stress that no broadening effects were included in the simulations. Similarly, the experimental echo responses from the unoriented samples of CSL in MBBA matrices, Fig.8, correspond closely to the simulated ones in the case of $\langle P_2 \rangle = 0$.

The echo responses observed from CSL molecules in eggPC matrices, Fig. 9, reveal significant amplitude modulations. This is in agreement with the extremely high degree of orientational order found from the CW-ESR spectra. In view of the fact that the modulations are clearly visible despite the effects of line broadening, we have simulated the echo responses using the parameters extracted from the CW-ESR lineshape analysis and included broadening effects, Fig. 9. The agreement between the simulations and experiments is satisfying.

CONCLUSIONS

We have here investigated the origin of the amplitude modulations of the Hahn echo responses from samples characterized by a high degree of orientational order. It is shown that the modulations arise from the use of soft pulses in the Hahn sequence. Soft pulses have a limited spectral range and cover only a small portion of the CW-ESR spectra, so that not all the spins are on-resonance. The magnetization vectors of the off-resonance spins only partially tilted away from the laboratory *z* axis, the direction of the applied static magnetic field. They thus contribute oscillating components to the magnetization in the *xy* plane. The contribution from the off-resonance spins to the Hahn echo formation is significant in highly oriented samples, but cancels out in samples exhibiting a small degree of order.

The experimental echo responses obtained from CSL molecules embedded in rigid matrices of eggPC bilayers and the liquid crystalline materials ZLI and MBBA confirm the theoretical predictions.

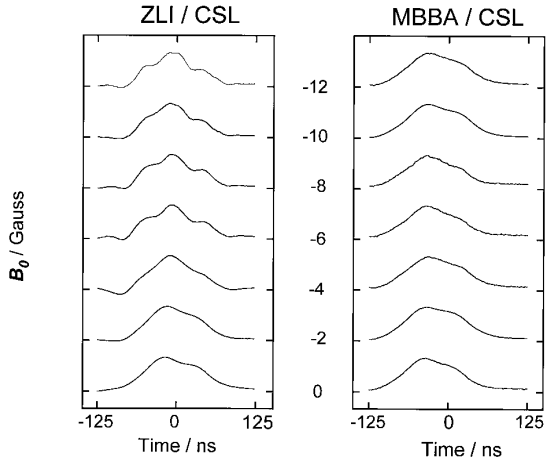

FIG. 8. Typical Hahn echo responses for several magnetic field positions from CSL in ZLI and MBBA matrices at $T = 160$ K. Every trace is an echo shape, with horizontally a time window around the echo maximum (250 ns) and vertically the magnetization along the *y* axis.

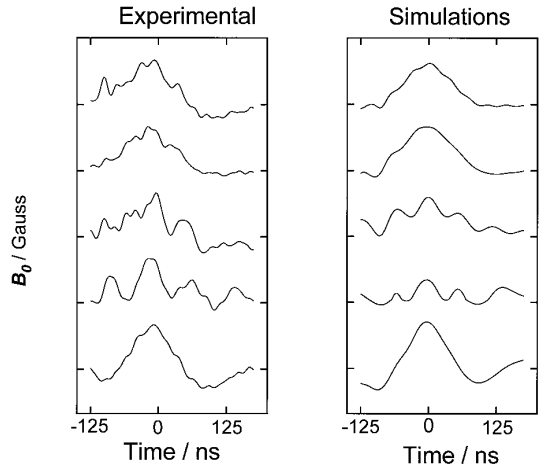

FIG. 9. Typical Hahn echo responses for several magnetic field positions from CSL in eggPC matrices at $T = 160$ K. Every trace is an echo shape, with horizontally a time window around the echo maximum (300 ns) and vertically the magnetization along the *y* axis. The parameters extracted from the analysis of the CW lineshapes, Table 1, were used in the simulations.

REFERENCES

1. C. van der Struijf, T. Ph. Pelupessy, E. E. van Faassen, and Y. K. Levine, *J. Magn. Reson. B* **111,** 158 (1996).
2. D. J. Bigelow and G. Inesi, *Biochim. Biophys. Acta* **1113,** 323 (1992).
3. G. R. Luckhurst and C. A. Veracini (Eds.), ''The Molecular Dynamics of Liquid Crystals,'' Kluwer Academic, Dordrecht (1994).
4. A. L. Lehninger, ''Biochemistry: The Molecular Basis of Cell Structure and Function,'' Worth Pub., New York (1970).
5. L. J. Korstanje, E. E. van Faassen, and Y. K. Levine, *Biochim. Biophys. Acta* **982,** 196 (1989).
6. J. Fessmann, N. Rösch, E. Ohmes, and G. Kothe, *Chem. Phys. Lett.* **152,** 491 (1988).
7. V. K. Dolganov, R. Fouret, C. Gors and M. More, *Phys. Rev. E* **49,** 5230 (1994).
8. W. Froncisz and J. S. Hyde, *J. Magn. Reson.* **47,** 515 (1982).

9. C. P. Poole, ''Electron Spin Resonance: A Comprehensive Treatise on Experimental Techniques,'' Interscience, New York (1967).

10. W. N. Hardy and L. A. Whitehead, *Rev. Sci. Instrum.* **52,** 213 (1982).

11. M. E. Rose, ''Elementary Theory of Angular Momentum,'' Wiley, New York (1957).

12. H. Eviatar, E. E. van Faassen, Y. K. Levine and D. I. Hoult, *Chem. Phys.* **181,** 369 (1994).

13. C. P. Slichter, ''Principles of Magnetic Resonance,'' Springer-Verlag, Berlin/New York (1990).

14. L. J. Libertini and O. H. Griffith, *J. Chem. Phys.* **53,** 1359 (1970).

15. S. P. Van, G. B. Birell and O. H. Griffith, *J. Magn. Reson.* **15,** 444 (1974).

16. J. H. Freed, *in* ''Spin Labelling, Theory and Applications,'' (L. J. Berliner, Ed.), Vol. 1, p. 117, Academic Press, New York (1976).

17. G. R. Luckhurst and A. Sanson, *Mol. Phys.* **24,** 1297 (1972).

18. W. H. Press, W. T. Vetterling, S. A. Teukolsky and B. P. Flannery, ''Numerical Recipes,'' Cambridge Univ. Press, Cambridge (1992).

19. D. M. Small, ''The Physical Chemistry of Lipids,'' Plenum, New York (1986).

20. G. L. Millhauser and J. H. Freed, *J. Chem. Phys.* **81,** 37 (1984).